Electronic Supplementary Material

ESM Methods

Study Participant Screening

Blood Chemistries

HbA1c, a lipid panel, a comprehensive metabolic panel, and a complete blood count were obtained from blood samples collected after an overnight fast on the morning of the screening visit in the WUSTL Clinical and Translational Research Unit (CTRU). All samples were analyzed by the CTRU Core Lab for Clinical Studies.

Oral glucose tolerance test (OGTT)

Each participant completed a two-hour, 75-gram OGTT after a 12-hour overnight fast during their screening visit in the WUSTL Clinical and Translational Research Unit (CTRU) (1). The test was administered by CTRU nursing staff and supervised by the study physician.

One-repetition Maximum (1RM) Strength Assessment

One repetition maximum strength was measured for leg press, chest press, seated row, pull down, knee extension, shoulder press, and biceps curl exercises on a Hoist (San Diego, CA, USA) single pod exercise machine according to guidelines established by the American College of Sports Medicine (2). The 1RM testing was administered by a licensed physical therapist within the WUSTL Clinical and Translational Research Unit (CTRU) at the end of the screening visit.

Daily Physical Activity Monitoring

Participants' daily physical activity was measured by using an ActiGraph (Pensacola, FL) GT3X+ accelerometer. The monitor was placed on the non-dominant wrist with a non-removable wristband by a licensed physical therapist after completion of all screening procedures and worn for 7 days prior to the lipid metabolism study.

Body Composition

Each participant underwent a whole-body dual energy X-ray absorptiometry (DXA) scan (Hologic Discovery GDR 1000/W, software version 12.6.2 OD; Waltham, MA) to assess regional and total lean body and fat masses (3). This test was administered by a licensed physical therapist and a certified DXA technologist within the Washington University in St. Louis (WUSTL) School of Medicine.

Lipid Metabolism Study

Cross-Over Procedures

For the order of conditions (rest>exercise vs exercise>rest) participants selected from 10 pieces of paper from a bowl (5 stating "rest>exercise" and 5 stating "exercise>rest") to ensure an equal number of participants in each order. The paper was not returned to the bowl to ensure that 5 participants were assigned to each order.

Standardized Meals

The composition of the standardized meals was as follows: breakfast: 2.18 MJ, 19% protein, 31% fat, 50% carbohydrates; lunch: 3.02 MJ, 19% protein, 32% fat, 49%

carbohydrates; afternoon snack: .75 MJ, 4% protein, 15% fat, 81% carbohydrates; and dinner: 3.26 MJ, 20% protein, 28% fat, 52% carbohydrates.

Liquid Test Meal

[1,1,1,2,2,2,3,3,3,4,4,4-$^{13}C_{12}$]tripalmitin (10 mg/kg body weight) was emulsified in lecithin (0.4 g) and vegetable oil (6.3 g); the emulsion was microwaved for 5 minutes to warm before being added to the liquid meal, which was again microwaved shortly, and then sonicated to evenly distribute the tracer. To ensure meal consistency for both the exercise and rest visits for each participant, a single meal was prepared and then divided in half. Participants consumed the liquid meal within 16 minutes (1/4 of the meal provided every 4 minutes). After each aliquot was consumed, the liquid meal containers were rinsed with 10 ml of water and the rinse was given to participants to ensure they ingested the entire study meal.

Exercise Protocol:

The exercise prescription used in this study (3 sets, 10-12 repetitions, 80% 1RM) was selected to be consistent with the recommendations of the American Diabetes Association, the American College of Sports Medicine, and the existing literature on resistance exercise for the treatment of type 2 diabetes 2,4). Since there is a positive correlation between energy expenditure and the reduction in postprandial TG, we selected a higher intensity to maximize the effects of the single exercise session (5).

Sample Processing

Blood samples were placed in chilled tubes containing EDTA and placed on ice. Plasma was recovered by low speed centrifugation within 30 min of sample collection. An aliquot of plasma (3 ml) was kept in the refrigerator for subsequent isolation of lipoprotein fractions by ultracentrifugation; the remaining plasma was frozen at -80°C for further processing. To separate the triglyceride-rich lipid (TRL) fraction, containing both chylomicrons and VLDL, two milliliters of each plasma sample was transferred into Optiseal tubes (Beckman Instruments, Inc., Palo Alto, CA), covered with a saline solution (d=1.006 g/ml), and centrifuged for 16 h at 8°C in a 50.4 Ti rotor (Beckman Instruments, Inc.) at 45,000 rpm (6). The top layer, containing TRL, was removed by tube slicing (Beckman Instruments, Inc.) (6). The exact volume that was recovered (~1.3 ml) was recorded, and the samples were stored at -80°C. Chylomicrons were recovered by over layering 1 ml of plasma with a d=1.006 g/ml saline solution, followed by ultracentrifugation at 16°C for 35 minutes in a SW41 swinging bucket rotor (Beckman Instruments, Palo Alto, CA) at 25,000 rpm (7).

The palmitate and glycerol tracer enrichments in triglycerides (TG) in the TRL and chylomicron fractions were determined by gas chromatography-mass spectrometry (GC/MS) after isolation of TG by thin layer chromatography as previously described (6). Briefly, heptane-diethyl ether-formic acid (80:20:2, v/v/v) and visualized with 0.01% rhodamine 6G. TLC scrapings containing TGs were recovered, extracted with chloroform-methanol (3:1, v/v), transferred to 13 mm screw-top vials and dried under vacuum. Fatty acid methyl esters (FAMEs) were prepared by adding 0.5 ml of 10% acetyl chloride in methanol, capping the tubes with Teflon-lined caps, incubated at 70°C for 30 min, and dried under vacuum. The glycerol liberated by the transmethylation

reaction was derivatized by the addition of 200 µl of 5% heptafluorobutyric (HFB) anhydride in ethyl acetate. Capped vials were incubated at 70°C for 30 min. After drying under vacuum, 100 µl ethyl acetate was added and samples were transferred to autosampler vials for GC-MS analysis of HFB- glycerol and palmitate methyl ester in the same run. Plasma glycerol and palmitate were recovered from 0.25 ml plasma after precipitation of plasma proteins with acetone and extraction of the aqueous phase with hexane. The aqueous phase containing glycerol was dried under vacuum (SpeedVac) and derivatized with 100 µl of HFB anhydride-ethyl acetate (1:1, v/v) at 70°C for 10 min. After drying in a SpeedVac, the samples were dissolved in 100 µl ethyl acetate.

The [$^{13}C_{16}$] palmitate (intravenously delivered) and [$^{13}C_4$]palmitate (meal-derived) enrichments were measured by GC/MS after instrument calibration with standards of known isotopic enrichment as previously described (6). Quantitative GC/MS was used to measure plasma free fatty acid (FFA) concentrations (8). Enrichments are expressed as tracer to tracee ratio (TTR) or mol percent enrichment (MPE) as appropriate for computation of kinetic parameters.

Skeletal Muscle Mitochondrial Respiration

6-10 mg (wet weight) of tissue were transferred into BIOPS solution (50 mM K^+-MES, 20 mM taurine, 0.5 mM dithiothreitol, 6.56 mM $MgCl_2$, 5.77 mM ATP, 15 mM phosphocreatine, 20 mM imidazole, pH 7.1, adjusted with 5N KOH at 0 °C, 10 mM Ca–EGTA buffer (2.77 mM CaK_2EGTA + 7.23 mM K_2EGTA; 0.1mM free calcium)) and then placed onto a glass plate where fibers were separated using forceps (11). To ensure complete permeabilization, the fibers were incubated by gentle agitation at 4°C in BIOPS

solution containing 50 μg/ml saponin for 20 min. Fibers were washed for 10 min at 4°C in ice-cold (MiR05; 0.5 mM EGTA, 3mM $MgCl_2 \cdot 6H_2O$, 20 mM taurine, 10 mM KH_2PO_4, 20 mM HEPES, 1g/L BSA, 60 mM potassium-lactobionate, 110 mM sucrose, pH 7.1) and the wet weight of the fibers was measured on a microbalance (Mettler Toledo, Greifensee, Switzerland) (11).

3 mg (wet weight) of permeabilized muscle fibers were used per respirometer chamber (Oxygraph-2k; Oroboros Instruments, Innsbruck, Austria) containing 2.090 ml MiR05 at 37°C. Oxygen concentration (μM) and oxygen flux (pmol s^{-1} mg^{-1}; negative time derivative of oxygen concentration, divided by muscle mass per volume) were recorded using DatLab software (Oroboros Instruments). The oxygen concentration in the chamber was maintained between 150 and 400 μM to avoid oxygen limitation of fiber respiration.

The substrate-uncoupler-inhibitor titration protocol was as follows (final concentrations): palmitoylcarnitine (0.05 mM), L-carnitine (5 mM), and malate (0.5 mM) to support electron entry from fatty acid β-oxidation through electron-transferring flavoprotein (ETF) and Complex I (CI) to coenzyme Q. Prior to the addition of ADP, oxygen utilization occurs due to proton slip across the inner mitochondrial membrane (LEAK respiration). ADP (4 mM) was then added to stimulate fatty-acid supported oxidative phosphorylation $(ETF + CI)_{Lip}$. The subsequent addition of pyruvate (10 mM) stimulates glycolytic oxidative phosphorylation. Glutamate (10 mM) was then added, followed by succinate (10 mM) to recapitulate the TCA cycle and stimulate maximal oxidative phosphorylation $[(ETF + CI + CII)_{Lip + Pyr}]$ through both ETC complex I and complex II. Cytochrome *c* (10 μM) is added to test the integrity of the outer

mitochondrial membrane. The increase of flux with cytochrome *c* was on average 3.3 ± 0.4%. Electron transfer system capacity (CI+II$_E$) was reached by stepwise (0.5 μM) addition of the uncoupler carbonylcyanide p-trifluoromethoxyphenylhydrazone (FCCP). Finally, the addition of rotenone (0.5 μM), an inhibitor of complex I was used to measure succinate-supported ETS capacity (CII$_E$). Figure 5 and Supplemental Table 1 outline the titration protocol and respiratory states included in this analysis. Supplemental Table 2 outlines the flux control and substrate control ratios calculated in this study.

Real-Time Polymerase Chain Reaction (RT-qPCR)

Total RNA was isolated from skeletal muscle and subcutaneous adipose tissue samples using Trizol reagent (#15596018; Invitrogen, Carlsbad, CA) and RNeasy mini kit (#74104; Qiagen, Valencia, CA) respectively (12). Total RNA was reverse transcribed into cDNA by using the High-Capacity cDNA Reverse Transcription Kit (#4368813; Invitrogen, Invitrogen, Carlsbad, CA) (12). The expression of each gene was determined by normalizing the Ct (cycle threshold) value of each sample to the housekeeping control gene, ribosomal protein (*RPLP0*) (12).

Plasma Lipid Kinetics Calculations

The concentrations of $^{13}C_4$-palmitate (meal-derived) and $^{13}C_{16}$-palmitate (intravenously infused) in TRL-TG and chylomicron-TG were calculated using the following equation[7]:

$$[^{13}C_4]\ or [^{13}C_{16}] palmitate\ concentration\ (\mu mol/L)$$

$$= \left(total\ TG \left(\frac{\mu mol}{l} \right) \times\ 3 \right.$$

$$\left. \times\ \%contribution\ of\ palmitate\ to\ the\ total\ TG\ fatty\ acid\ pool\ x\ [MPE\ ^{13}C_4\ \ or\ ^{13}C_{16} palmitate] \right)$$

Accordingly, the free $^{13}C_4$ and $^{13}C_{16}$-palmitate concentrations in plasma were calculated by multiplying the plasma FFA concentration by the % contribution of palmitate to total FFA and the $^{13}C_4$ or $^{13}C_{16}$-palmitate MPE (8). The concentrations of $^{13}C_4$-palmitate and $^{13}C_{16}$-palmitate in VLDL-TG were calculated by subtracting the respective tracer concentrations in chylomicron TGs from that in TRL-TG (chylomicrons plus VLDL). Insulin sensitivity (HOMA-%S), and beta cell function (HOMA-%B) were calculated using the HOMA 2 model (10).

For variables where values decreased from baseline during the postprandial period, the calculated incremental AUC is negative and represents the area above the curve extending up to the baseline value, providing an index of postprandial suppression.

Statistical Analysis and Sample Size Determination

Data were analyzed for normality using the Shapiro-Wilk test. Box plots were visually inspected and measures of the mean, median, skewness, and kurtosis were used to evaluate deviation form normality. In cases where non-normality was suspected, statistics were re-calculated using non-parametric equivalents. AUCs, respiration, lipid oxidation, and gene expression measures were analyzed as outlined by Wellek and Blettner (13). T

Effect sizes reported from previous literature for secondary outcomes in this study were consistent with those reported for the primary outcome, including: 1) differences

between exercise and rest on lipoprotein turnover (effect sizes ranging from 2.0-3.75 on basal VLDL-FCR after resistance exercise) (14,15); 2) FFA Ra (effect sizes ranging from 1.5-6.0 after aerobic exercise) (16,17); 3) FFA Rd (effect sizes ranging from 3-4.4 after aerobic exercise) (18,19); 4) lipid oxidation (effect sizes reported from 1.01-2.89 after a single bout of resistance exercise) (20,21), 5) mitochondrial respiration (effect size estimates of 1.02-3.0 after resistance exercise training) (22,23); 6) skeletal muscle lipid metabolism gene expression (effect sizes ranging from 0.61-2.65 for skeletal muscle PGC1alpha expression after acute resistance exercise) (24,25); and 7) adipose tissue lipid metabolism gene expression (with a previous study finding statistically significant increases in PDK4, HSL, ATGL, and CD36 with n=9 one hour after a single bout of aerobic exercise) indicating that 10 participants would be sufficient to achieve at least 80% power at an alpha=.05 for paired differences between rest and exercise on these variables (26).

ESM Table 1. Substrate-uncoupler-inhibitor titration (SUIT) protocol (27)

Definition	Abbreviation	Flux State	Titration
Leak	$(ETF + CI)_{LEAK}$	L	PC + Mal
FFA Oxidation through CI	$(ETF + CI)_{Lip}$		PC + Mal + ADP
Combined FFA and Pyruvate Oxidation Through CI	$(ETF + CI)_{Lip+Pyr}$		PC + Mal + ADP + Pyr + Glut
Max OXPHOS	$(ETF + CI + CII)_{Lip+Pyr}$	P	PC + Mal + ADP + Pyr + Glut + Succ
Maximal ETS	$(ETF + CI + CII)_{E}$	E	PC + Mal + ADP + Pyr + Glut + Succ + FCCP
CII Supported Respiration	$(CII)_{E}$		PC + Mal + ADP + Pyr + Glut + Succ + FCCP + Rot

FFA = free fatty acids. P and OXPHOS = oxidative phosphorylation (coupled respiration). E and ETS = electron transport chain capacity/uncoupled respiration. ETF = electron transport flavoprotein. CI = electron transport chain complex I. L and LEAK = leak respiration. Lip = respiration in response to palmitoylcarnitine titration. CII = electron transport chain complex II. PC = palmitoylcarnitine, Mal = malate. Pyr = pyruvate. Glut = glutamate. Succ = succinate. FCCP = Carbonyl cyanide-4-(trifluoromethoxy)phenylhydrazone. Rot = rotenone.

ESM Table 2. Flux control and substrate control ratios

Measure	Calculation
Flux Control Ratios	
Leak Control[27]	L/E
OXPHOS Control Ratio[27]	P/E
Respiratory Acceptor Control Ratio[27]	P/L
L/P Ratio[28]	L/P
Substrate (Pathway) Control Ratios[27]	
CI Lipid Normalized to Max OXPHOS	$(ETF + CI)_{Lip}$ /P
CI Lipid + Pyruvate Normalized to Max OXPHOS	$(ETF + CI)_{Lip+Pyr}$ /P
CI Lipid Normalized to Max ETS Capacity	$(ETF + CI)_{Lip}$ /E
CI Lipid + Pyruvate Normalized to Max ETS capacity	$(ETF + CI)_{Lip+Pyr}$ / E
CII Respiration normalized to Max OXPHOS	$(CII)_{E}$ /P
CII Respiration normalized to Max ETS Capacity	$(CII)_{E}$/ E
Other	
Lipid/Glucose Balance	$(ETF + CI)_{Lip}$/ (($(ETF + CI)_{Lip+Pyr}$ - $(ETF + CI)_{Lip}$)
ETS Coupling Efficiency[29]	(E-L)/E
Excess E-P Capacity (E-P)[27]	E-P
Excess E-P Capacity Ratio (E-P/E)[30]	(E-P/E)
Free OXPHOS Capacity (P-L)[30]	(P-L)
Net OXPHOS Control Ratio (P-L)/E[30]	(P-L)/E

P and OXPHOS = oxidative phosphorylation (coupled respiration). E and ETS = electron transport chain capacity/uncoupled respiration. ETF = electron transport flavoprotein. CI = electron transport chain complex I. L and LEAK = leak respiration. Lip = respiration in response to palmitoylcarnitine titration. CII = electron transport chain complex II. PC = palmitoylcarnitine, Mal = malate. Pyr = pyruvate.

ESM Table 3. Sequence of primers used for RT-PCR

Gene	Accession No.	Forward (F) and reverse (R) primer
FOXO1	NM_002015	F: 5'- TCGTCATAATCTGTCCCTACACA -3' R: 5'- CGGCTTCGGCTCTTAGCAAA -3'
PPARGC1A	NM_013261	F: 5'- TCTGAGTCTGTATGGAGTGACAT -3' R: 5'- CCAAGTCGTTCACATCTAGTTCA -3'
PDK4	NM_002612	F: 5'- GGAGCATTTCTCGCGCTACA -3' R: 5'- ACAGGCAATTCTTGTCGCAAA -3'
LPL	NM_000237	F: 5'- TCATTCCCGGAGTAGCAGAGT -3' R: 5'- GGCCACAAGTTTTGGCACC -3'
SREBF1	NM_001005291	F: 5'- ACAGTGACTTCCCTGGCCTAT -3' R: 5'- GCATGGACGGGTACATCTTCAA -3'
MURF1	NM_032588	F: 5'- CTTCCAGGCTGCAAATCCCTA -3' R: 5'- ACACTCCGTGACGATCCATGA -3'
CD36	NM_000072	F: 5'- ATGTTGGAGCATTTGATTGAAAAAT -3' R: 5'- AGGAAATGAACTGATGAGTCACAGA -3'
HSL	NM_005357	F: 5'- AGTTAAGTGGGCGCAAGTC -3' R: 5'- GGTCAGGTTCTTGAGGGAAT -3'
ATGL	NM_020376	F: 5'- ACGTGGAACATCTCGTTCG -3' R: 5'- CTTCCGGGCCTCTTTAGATAC -3'
ADIPOQ	NM_001177800	F: 5'- GGCTTTCCGGGAATCCAAGG -3' R: 5'- TGGGGATAGTAACGTAAGTCTCC -3'
RPLP0	NM_001002	F: 5'- GTGATGTGCAGCTGATCAAGACT -3' R: 5'- GATGACCAGCCCAAAGGAGA -3'
FASN	NM_004104	F: 5'- TGGAAGTCACCTATGAAGCCA -3' R: 5'- ACGAGTGTCTCGGGGTCTC -3'
ACACA	NM_198838	F: 5'- ATGTCTGGCTTGCACCTAGTA -3' R: 5'- CCCCAAAGCGAGTAACAAATTCT -3'
CD36	NM_001001548	F: 5'- ATGTTGGAGCATTTGATTGAAAAAT -3' R: 5'- AGGAAATGAACTGATGAGTCACAGA-3'
CPT1A	NM_001876	F: 5'- TCCAGTTGGCTTATCGTGGTG -3' R: 5'- TCCAGAGTCCGATTGATTTTTGC -3'
CPT1B	NM_004377	F: 5'- GCGCCCCTTGTTGGATGAT -3' R: 5'- CCACCATGACTTGAGCACCAG -3'

Electronic Supplemental Results

ESM Table 4. Effect of exercise on flux and substrate control ratios (n=9)

Measure	Rest	Exercise	P-value	Effect Size
Flux Control Ratios				
Leak Control	0.08 ± 0.01	0.07 ± .003	0.73	0.12
OXPHOS Control Ratio	0.82 ± 0.07	0.92 ± 0.07	0.04	0.88
Respiratory Acceptor Control Ratio	12.0 ± 1.4	14.8 ± .83	0.03	0.94
L/P Ratio	0.10 ± 0.03	0.09 ± 0.02	0.33	0.36
Substrate Control Ratios				
CI Lipid Normalized to Max OXPHOS	0.29 [0.23-0.49; 0.08]	0.34 [0.24-0.60; 0.10]	0.04	0.53
CI Lipid + Pyruvate Normalized to Max OXPHOS	0.54 ± 0.02	0.55 ± 0.03	0.45	0.28
CI Lipid Normalized to Max ETS Capacity	0.25 ± 0.02	0.31 ± 0.01	0.01	1.20
CI Lipid + Pyruvate Normalized to Max ETS capacity	0.45 ± 0.04	0.49 ± 0.03	0.10	0.65
CII Respiration normalized to Max OXPHOS	0.67 [0.25-1.26; 0.37]	0.56 [0.49-1.3; 0.23]	0.26	0.28
CII Respiration normalized to Max ETS Capacity	0.58 ± 0.03	0.56 ± 0.02	0.46	0.25
Other				
Lipid/Glucose Balance	0.41 [0.31-0.99; 0.16]	0.52 [0.35-1.53; 0.41]	0.04	0.52
ETS Coupling Efficiency	0.92 ± 0.01	0.93 ± .003	0.73	0.13
Excess E-P Capacity (E-P) (pmol O_2·mg wt wt^{-1})	7.9 ± 3	5.9 ± 5.7	0.61	0.19
Excess E-P Capacity Ratio (E-P/E)	0.15 ± 0.07	0.08 ± 0.08	0.11	0.63
Free OXPHOS Capacity (P-L) (pmol O_2·mg wt wt^{-1})	60.7 ± 10.8	80.6 ± 12.8	0.01	1.07
Net OXPHOS Control Ratio (P-L)/E	0.86 [0.32-0.93; 0.25]	0.93 [0.35-1.10; 0.24]	0.07	0.46

Values are mean ± SE (normally distributed) or median [minimum-maximum; interquartile range] (non-normally distributed). P and OXPHOS = oxidative phosphorylation (coupled respiration). E and ETS = electron transport chain capacity/uncoupled respiration. ETF = electron transport flavoprotein. CI = electron transport chain complex I. L and LEAK = leak respiration. Lip = respiration in response to palmitoylcarnitine titration. CII = electron transport chain complex II. PC = palmitoylcarnitine, Mal = malate. Pyr = pyruvate. mg wt wt^{-1} = milligram wet weight of muscle tissue. P-value calculated for paired t-tests (parametric) or Wilcoxon Signed Rank test (non-parametric). Effect size = cohen's d (paired t-test) or r (Wilcoxon Signed Rank test).

.

ESM Figure 1. $^{13}C_4$-palmitate and $^{13}C_{16}$-palmitate TTR in Chylomicron-TG, TRL-TG, and Plasma Free Palmitate.

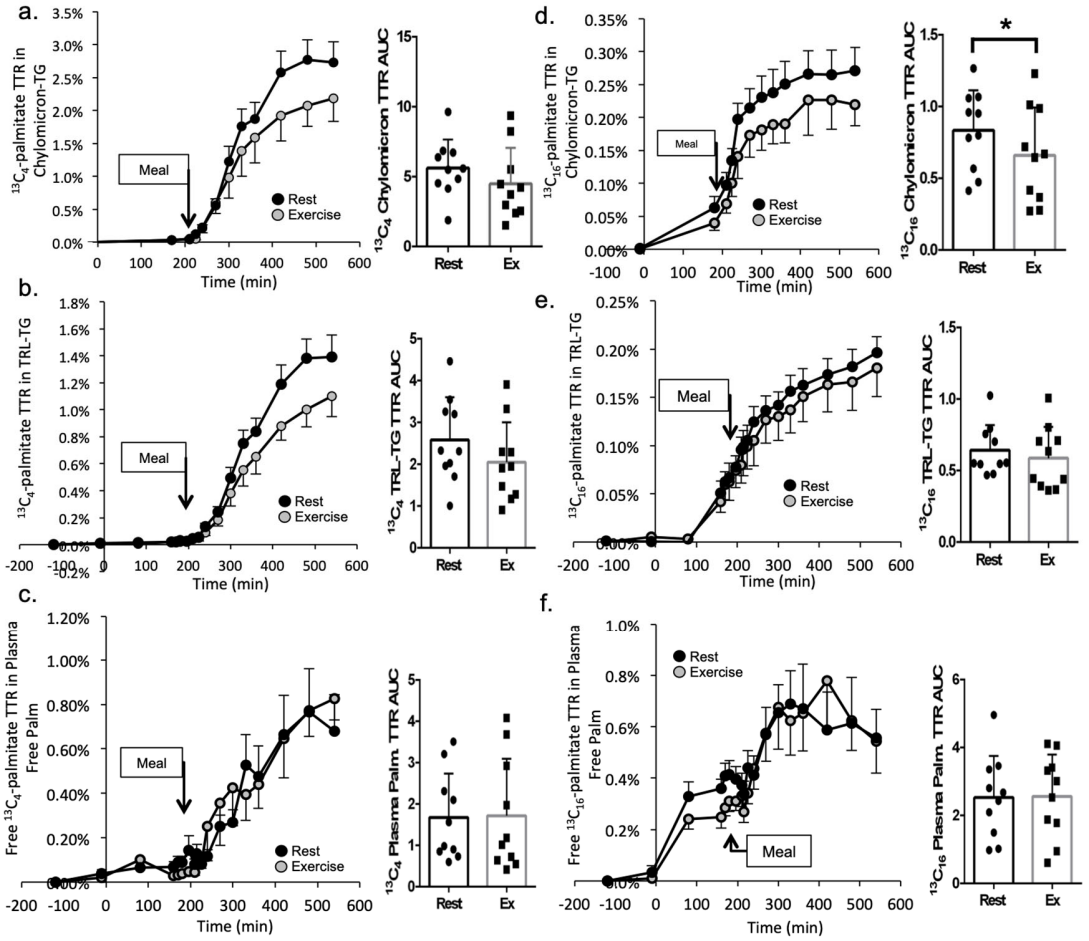

Time-course values are mean ± SE. Black circles = rest condition. Gray circles = exercise condition. The $^{13}C_4$-palmitate TTR is shown for Chylomicron-TG (a), TRL-TG (b), and free in plasma (c). The $^{13}C_{16}$-palmitate TTR is shown for Chylomicron-TG (d), TRL-TG (e), and free in plasma (f). TTR AUC (mean ± SD) is reported for each variable to the right in a-f. * denotes significant difference between rest and resistance exercise at $p<0.05$ for paired *t*-tests

Supplemental Works Cited

1. Magkos F, Fraterrigo G, Yoshino J, et al (2016) Effects of Moderate and Subsequent Progressive Weight Loss on Metabolic Function and Adipose Tissue Biology in Humans with Obesity. Cell Metab 23(4):591–601. doi:10.1016/j.cmet.2016.02.005
2. American College of Sports Medicine; Johnson EP, ed. ACSM's Guidelines for Exercise Testing and Prescription. 6th ed. Philadelphia, Pa: Lippincott Williams & Wilkins; 2000.
3. Bittel DC, Bittel AJ, Tuttle LJ, et al (2015) Adipose tissue content, muscle performance and physical function in obese adults with type 2 diabetes mellitus and peripheral neuropathy. J Diabetes Complications 29(2): 250-257. doi:10.1016/j.jdiacomp.2014.11.003
4. Colberg SR, Sigal RJ, Yardley JE, et al (2016) Physical activity/exercise and diabetes: a position statement of the American Diabetes Association. Diabetes Care 39:2065–79.10.2337/dc16-1728
5. Singhal A, Trilk JL, Jenkines NT, Bigelman KA, Cureton KJ (2009) Effect of intensity of resistance exercise on postprandial lipemia; J Appl Physiol (1985). Mar;106(3):823-9. doi: 10.1152/japplphysiol.90726.2008. Epub 2009 Jan 15
6. Patterson BW, Mittendorfer B, Elias N, Satyanarayana R, Klein S (2002) Use of stable isotopically labeled tracers to measure very low density lipoprotein-triglyceride turnover. J Lipid Res 43: 223–233
7. Park Y, Grellner WJ, Harris WS, Miles JM (2000) A new method for the study of chylomicron kinetics in vivo. Am J Physiol Endocrinol Metab Dec;279(6):E1258-63.
8. Patterson BW, Zhao G, Elias N, Hachey DL, Klein S (1999) Validation of a new procedure to determine plasma fatty acid concentration and isotopic enrichment. J Lipid Res. Nov; 40(11):2118-24.
9. Davitt PM, Arent SM, Tuazon MA, Golem DL, Henderson GC (2013) Postprandial triglyceride and free fatty acid metabolism in obese women after either endurance or resistance exercise. J Appl Physiol 114: 1743– 1754, 2013.
10. Song YS, Hwang YC, Ahn HY, Park CY (2016) Comparison of the usefulness of the updated homeostasis model assessment (homa2) with the original HOMA1 in the prediction of type 2 diabetes mellitus in Koreans. Diabetes Metab J 40(4):318–325.
11. Cardinale DA, Gejl KD, Ørtenblad N, Ekblom B, Blomstrand E, Larsen FJ (2018) Reliability of maximal mitochondrial oxidative phosphorylation in permeabilized fibers from the vastus lateralis employing high-resolution respirometry. Physiol Rep 6(4):e13611. doi:10.14814/phy2.13611
12. Yoshino J, Conte C, Fontana L, et al (2012) Resveratrol supplementation does not improve metabolic function in nonobese women with normal glucose tolerance. Cell Metab 16:658–664
13. Wellek S, Blettner M (2012) On the proper use of the crossover design in clinical trials: part 18 of a series on evaluation of scientific publications. Deutsches Ärzteblatt International 109(15):276-281. doi:10.3238/arztebl.2012.0276.

14. Egli L, Lecoultre V, Theytaz F, et al (2013) Exercise prevents fructose-induced hypertriglyceridemia in healthy young subjects. *Diabetes*. 62(7):2259–2265. doi:10.2337/db12-1651
15. Magkos F, Tsekouras YE, Prentzas KI, et al (2008) Acute exercise-induced changes in VLDL-triglyceride kinetics leading to hypotriglyceridemia manifest more readily after resistance than endurance exercise. *J Appl Physiol*. 105: 1228-1236
16. Magkos F, Patterson BW, Mohammed BS, Mittendorfer B (2009) Basal adipose tissue and hepatic lipid kinetics are not affected by a single exercise bout of moderate duration and intensity in sedentary women. *Clin Sci (Lond)*. 116(4):327–334. doi:10.1042/CS20080220
17. Henderson GC, Fattor JA, Horning MA, et al (2007) Lipolysis and fatty acid metabolism in men and women during the postexercise recovery period. *J Physiol*. 584(Pt 3):963–981. doi:10.1113/jphysiol.2007.137331
18. Horowitz JF, Klein S (2000) Oxidation of nonplasma fatty acids during exercise is increased in women with abdominal obesity. J Appl Physiol (1985). Dec;89(6):2276-82.
19. van Loon LJ, Greenhaff PL, Constantin-Teodosiu D, Saris WH, Wagenmakers AJ (2001) The effects of increasing exercise intensity on muscle fuel utilisation in humans. *J Physiol* 536(Pt 1):295–304. doi:10.1111/j.1469-7793.2001.00295.x
20. Frawley K, Greenwald G, Rogers RR, Petrella JK, Marshall MR (2018) Effects of Prior Fasting on Fat Oxidation during Resistance Exercise. *Int J Exerc Sci*. 11(2):827–833. Published 2018 Jun 1.
21. Farinatti P, Castinheiras Neto AG, Amorim PR (2016) Oxygen Consumption and Substrate Utilization During and After Resistance Exercises Performed with Different Muscle Mass. *Int J Exerc Sci*. 9(1):77–88. Published 2016 Jan 15.
22. Porter C, Reidy PT, Bhattarai N, Sidossis LS, Rasmussen BB (2015) Resistance Exercise Training Alters Mitochondrial Function in Human Skeletal Muscle. *Med Sci Sports Exerc* 47(9):1922–1931. doi:10.1249/MSS.0000000000000605
23. Salvadego D, Domenis R, Lazzer S, et al (2013) Skeletal muscle oxidative function in vivo and ex vivo in athletes with marked hypertrophy from resistance training. J Appl Physiol (1985) Jun;114(11):1527-35. doi: 10.1152/japplphysiol.00883.2012.
24. Schwarz NA, McKinley-Barnard SK, Spillane MB, Andre TL, Gann JJ, Willoughby DS (2016) Effect of resistance exercise intensity on the expression of PGC-1α isoforms and the anabolic and catabolic signaling mediators, IGF-1 and myostatin, in human skeletal muscle. Appl Physiol Nutr Metab 41(8):856-63. doi: 10.1139/apnm-2016-0047.
25. Nygaard H, Slettaløkken G, Vegge G, et al. (2015) Irisin in blood increases transiently after single sessions of intense endurance exercise and heavy strength training. *PLoS One* 10(3):e0121367. doi:10.1371/journal.pone.0121367
26. Chen YC, Travers RL, Walhin JP et al (2017) Feeding influences adipose tissue responses to exercise in overweight men. Am J Physiol Endocrinol Metab. Jul 1;313(1):E84-E93. doi: 10.1152/ajpendo.00006.2017.
27. Gnaiger E. Mitochondrial pathways and respiratory control. An introduction to OXPHOS analysis. 4th ed. 2014. Mitochondr Physiol Network 19.12. Oroboros

MiPNet Publications, Innsbruck:80 pp
28. Gnaiger E (2009) Capacity of oxidative phosphorylation in human skeletal muscle: new perspectives of mitochondrial physiology. Int J Biochem Cell Biol Oct; 41(10):1837-45
29. Gnaiger E. Cell ergometry: OXPHOS and ETS coupling efficiency. Mitochondr Physiol Network. 2015-01-18.
30. Burtscher J, Zangrandi L, Schwarzer C, Gnaiger E (2015) Differences in mitochondrial function in homogenated samples from healthy and epileptic specific brain tissues revealed by high-resolution respirometry. Mitochondrion Nov; 25:104-12.